Journal of Vibration and Control
http://jvc.sagepub.com/

Semi-active Vibration Control Schemes for Suspension Systems Using Magnetorheological Dampers

Y. Shen, M. F. Golnaraghi and G. R. Heppler

Journal of Vibration and Control 2006 12: 3
DOI: 10.1177/1077546306059853

The online version of this article can be found at:
http://jvc.sagepub.com/content/12/1/3

Published by:
SAGE
http://www.sagepublications.com

Additional services and information for *Journal of Vibration and Control* can be found at:

Email Alerts: http://jvc.sagepub.com/cgi/alerts

Subscriptions: http://jvc.sagepub.com/subscriptions

Reprints: http://www.sagepub.com/journalsReprints.nav

Permissions: http://www.sagepub.com/journalsPermissions.nav

Citations: http://jvc.sagepub.com/content/12/1/3.refs.html

>> Version of Record - Feb 2, 2006

What is This?

Downloaded from jvc.sagepub.com at PENNSYLVANIA STATE UNIV on March 2, 2014

Semi-active Vibration Control Schemes for Suspension Systems Using Magnetorheological Dampers

Y. SHEN
Department of Mechanical Engineering, University of Waterloo, Waterloo, Ontario, Canada, N2L 3G1 (y6shen@engmail.uwaterloo.ca)

M. F. GOLNARAGHI
Mechatronic and Smart Material Systems, Department of Mechanical Engineering, University of Waterloo, Waterloo, Ontario, Canada, N2L 3G1

G. R. HEPPLER
Department of Systems Design Engineering, University of Waterloo, Waterloo, Ontario, Canada, N2L 3G1

(Received 28 December 2004; accepted 16 August 2005)

Abstract: Three semi-active control methods are investigated for use in a suspension system using a commercial magnetorheological damper. The three control methods are the limited relative displacement method, the modified skyhook method, and the modified Rakheja–Sankar method. The method of averaging has been adopted to provide an analytical platform for analyzing the performance of the different control methods. The analytical results are verified using numerical simulation, and further are used to assess the efficiency of different control methods. An experimental test bed has been developed to examine the three control methods under sinusoidal and random excitations. Both analytical and experimental results confirm that the Rakheja–Sankar control and modified skyhook control methods significantly reduce the root-mean-square response of both the acceleration and relative displacement of the sprung mass, while the limited relative displacement controller can only control the relative displacement of the suspension system.

Key Words: Magnetorheological damper, semi-active control, suspension system, averaging method

1. INTRODUCTION

For vehicle suspension system design, it is always challenging to maintain simultaneously a high standard of ride, handling, and body attitude control under all driving conditions. The problems stem from the wide range of operating conditions created by varying road conditions, vehicle speed, and load. In general, during cornering, braking, and bumping, a high stiffness and damping is needed to provide good handling properties, and to satisfy workspace limitations of the suspension system. However, when a vehicle runs on a low roughness road, a suspension system with low stiffness and damping is needed for good

Journal of Vibration and Control, **12(1):** 3–24, 2006 DOI: 10.1177/1077546306059853
©2006 SAGE Publications
Figures 2, 3, 5, 8, 11 appear in color online: http://jvc.sagepub.com

Downloaded from jvc.sagepub.com at PENNSYLVANIA STATE UNIV on March 2, 2014

ride comfort. A good suspension system should provide good vibration isolation, i.e. small acceleration of the body mass, and a small "rattle space", which is the maximal allowable relative displacement between the vehicle body and various suspension components (Hrovat et al., 1988).

There are three broad classifications of suspension systems: passive, active, and semi-active. Each of these types of suspension has different advantages and disadvantages.

Passive vibration control involves an inherent compromise between low-frequency and high-frequency vibration isolation. Passive suspension systems are subject to various trade-offs when they are excited across a large frequency bandwidth. Compared with passive control, active control can improve the performance over a wide range of frequencies. However, active vibration control has the disadvantages of complexity and high-energy consumption. Semi-active control has shown many advantages in vehicle suspension systems due to its low energy consumption with similar vibration control performance to the active control methods. A semi-active control method maintains the reliability of passive control methods and, yet, includes the advantage of the adjustable parameter characteristics of active systems.

In this paper, several semi-active dampers have been proposed. The devices include variable orifice dampers, adjustable tuned liquid dampers, and controllable fluid dampers (Dyke et al., 1998). However, these semi-active dampers have a relatively low response speed. From control theory, a large time delay makes the control system inefficient and even tends to make the system unstable. In recent years, magnetorheological (MR) dampers have received much attention as semi-active system actuators for their rapid response to the applied magnetic field and their compact size. The MR effect was first observed by Rabinow (1948) and was initially defined as the magnetically induced fibrillation of micrometer-sized magnetizable particles suspended in low viscosity fluid. Without the magnetic field effect, the MR fluid has the properties of a Newtonian fluid; however, when the MR fluid is under the effect of a magnetic field the particles align themselves with respect to the magnetic field and form into chains or columns, which makes the viscosity of the MR fluid change. The damping force of an MR damper is a hysteretic force that can be modeled by either the Bouc–Wen model or by other hysteresis molds.

Several semi-active control methods have been proposed. Dyke et al. (1998) applied a clipped-optimal control strategy (LQG) based on acceleration feedback. The performance of LQG or LQR controllers is dependent upon the choice of weighting matrices for the vector of regulated responses and control forces. When the cost function weighting matrices are changed, the response of the system can be greatly changed and the values in the weighting matrices are often determined by trial and error.

Leitmann (1995) applied Lyapunov's direct approach, which reduces the response by minimizing the cost function and the rate of change of a Lyapunov function, to design a semi-active controller. Kim and Lee (2003) applied this same method to a multi-degrees-of-freedom suspension system. Choi et al. (2001) and Yao et al. (2002) used a semi-active skyhook controller to control an electrorheological (ER) and an MR suspension system, respectively. Boggs et al. (2004) investigated the energy dissipation of an MR damper in a quarter-car rig under a semi-active hybrid control policy. The hybrid control is a linear combination of skyhook and ground hook control. Lai and Liao (2002) developed a sliding mode controller theory for a suspension system with an MR damper.

Several semi-active control methods have been identified in the prior art. Most of these studies have focused only on numerical simulation studies, without any experimen-

Downloaded from jvc.sagepub.com at PENNSYLVANIA STATE UNIV on March 2, 2014

tal confirmation, or without analytical treatment of nonlinear system equations. The reasons may possibly be attributed to the complexity of the control methods, which may not be realizable in real time, or some of the state variables may not be directly measured and accurately obtained through an observer. From this point of view, practical and easy to use control methods need to be developed for application on real suspension systems.

In this paper, we suggest and investigate three semi-active control methods. They are the limited relative displacement (LRD) method, the modified Rakheja–Sankar (R–S) method (Rakheja and Sanker, 1985), and the modified skyhook control (MSK) method. The LRD method is designed to the limit the relative displacement between the sprung mass and the base to control the working space of the suspension system. The modified R–S method minimizes the damping force when it is in the same direction as the spring force, and maximizes the damping force when it acts opposite to the spring force. Because this method needs only one LVDT sensor it allows for a low cost implementation. In general, the original MSK method needs to determine the absolute velocity of the sprung mass; however, it is difficult to obtain the absolute velocity from a measured acceleration of the sprung mass so the MSK method has been developed. The MSK method does not require the absolute velocity of the sprung mass, but instead uses the jerk of the sprung mass to indirectly determine the direction of the sprung mass absolute velocity.

The characteristics of the three suggested semi-active control methods are determined by using the method of averaging when the damping force is regarded as piecewise linear. This analytical approach obtains a closed-form system frequency response formula, and provides an easy way to study the efficacy of the different control methods. Numerical simulation is used to verify the results obtained from the averaging method.

An experimental test bed is used to verify the three control methods when the system is excited with a swept sine and random excitation.

2. THREE CONTROL STRATEGIES

In the simplest approach to evaluate the vibration control efficiency of different control strategies, a one-degree-of-freedom (1DOF) quarter-car model, as shown in Figure 1, has been adopted.

2.1. Limited Relative Displacement Control Method

The ideal goal of an optimal suspension is to minimize the sprung mass relative displacement and acceleration. However, these two criteria are in conflict. In general, a suspension system with a small relative displacement corresponds to a high sprung mass acceleration, and a large relative displacement corresponds to a low sprung mass acceleration. For this reason, we set our control strategy in a way that the MR damper is switched to a high damping ratio when the relative displacement is higher than a specific value and a low damping value otherwise. This on–off control law can be expressed as

$$\zeta_s = \begin{cases} \zeta_{\max} & |x_s - y| \geq \delta \\ \zeta_{\min} = 0 & |x_s - y| < \delta \end{cases} \tag{1}$$

Downloaded from jvc.sagepub.com at PENNSYLVANIA STATE UNIV on March 2, 2014

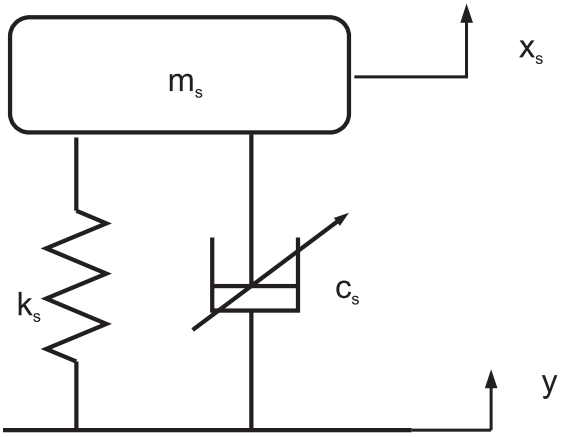


Figure 1. 1DOF suspension system.

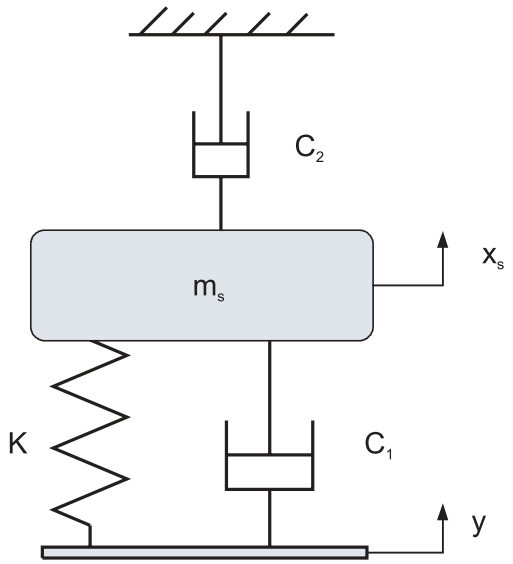


Figure 2. Schematic structure of skyhook control system.

where ζ_s is the equivalent damping ratio of the suspension system. This method can limit the relative displacement of the suspension by adjusting two parameters, $\zeta_{\max}$ and δ.

2.2. Modified Skyhook Control Method

Skyhook control is a popular and effective vibration control method because it can dissipate system energy at a high rate. A typical skyhook physical model is shown in Figure 2 where the damping force provided by damper C_2 always opposes the absolute velocity of m_s.

Downloaded from jvc.sagepub.com at PENNSYLVANIA STATE UNIV on March 2, 2014

According to the skyhook working principle, the semi-active on–off control law is

$$\zeta_s = \begin{cases} \zeta_{\max} & \dot{x}_s(\dot{x}_s - \dot{y}) \geq 0 \\ 0 & \dot{x}_s(\dot{x}_s - \dot{y}) < 0. \end{cases} \tag{2}$$

The relative velocity $(\dot{x}_s - \dot{y})$ can be obtained by differentiating the measured relative displacement between the sprung mass and the base. However, the absolute velocity $\dot{x}_s$ is impossible to measure for a running vehicle. In general, we can only measure the acceleration of the sprung mass. Hedrick et al. (1994) suggested that the absolute sprung mass velocity $\dot{x}_s$ cannot be estimated in an exponentially stable manner. It could theoretically be obtained by integrating the acceleration of the sprung mass and passing the result through a high-pass filter to remove the direct current (DC) offset. In practice, this is difficult to do because the acceleration offset is not constant and the initial condition of the integral is hard to be determined. For these reasons, we modified the control law (2) to the form

$$\zeta_s = \begin{cases} \zeta_{\max} & \dddot{x}_s(\dot{x}_s - \dot{y}) \leq 0 \\ 0 & \ddot{x}_s(\dot{x}_s - \dot{y}) > 0 \end{cases} \tag{3}$$

where the jerk $\dddot{x}_s$ of the sprung mass can be obtained by differentiating the filtered acceleration of the sprung mass. Obviously for a sinusoidal input, the phase difference between the jerk $\dddot{x}_s$ and $\dot{x}_s$ is π in this case, which is different from the skyhook techniques in the prior art. This control algorithm makes the MSK method easier to implement in a practical system without using a complex observer.

2.3. Modified Rakheja–Sankar Control Method

Rakheja and Sankar (1985) noticed that the damping force in a passive damper tends to increase the sprung mass acceleration when the damping force is in the same direction as the spring force. A semi-active damper should ideally have no damping force, or at least a minimal damping force, when the spring force and damping force have same direction. According this concept, Alanoly and Sankar (1987) suggested an on–off control strategy where the damping force is set to zero when the damping force and spring force are in the same direction and the damping force is adjusted to balance the spring force when they act in the opposite direction. Mathematically, this can be expressed as

$$F_d = \begin{cases} -\alpha k(x_s - y) & (x_s - y)(\dot{x}_s - \dot{y}) \leq 0 \\ 0 & (x_s - y)(\dot{x}_s - \dot{y}) > 0. \end{cases} \tag{4}$$

In practice, it is hard to make the damping force fully follow the spring force, so the above control strategy is modified to a new form, which can be expressed as

$$\zeta_s = \begin{cases} \zeta_{\max} & (x_s - y)(\dot{x}_s - \dot{y}) \leq 0 \\ 0 & (x_s - y)(\dot{x}_s - \dot{y}) > 0. \end{cases} \tag{5}$$

Downloaded from jvc.sagepub.com at PENNSYLVANIA STATE UNIV on March 2, 2014

This control method only needs measurement of the relative motion between the sprung mass and the base. The relative velocity can be obtained by differentiating the relative displacement. It is possible to make the system simple in structure.

3. ANALYSIS OF THE CONTROLLERS USING THE AVERAGING METHOD

The 1DOF suspension system controlled with any of the above three control strategies is a piecewise nonlinear system. Here, we adopt the averaging method to analyze the properties of each semi-active control method.

The governing equation of the 1DOF system, shown in Figure 1, is

$$m_s\ddot{x}_s + k_s(x_s - y) + F_d = 0, \tag{6}$$

where F_d is the damping force. Assuming base excitation $y = y_0\cos(\omega t)$ and introducing time scaling $\tau = \omega t$, $\omega_s = \sqrt{k_s/m_s}$ defining $x_r = x_s - y$ and $r = \omega/\omega_s$, equation (6) becomes

$$r^2\frac{\mathrm{d}^2x_r}{\mathrm{d}\tau^2} + x_r + 2\zeta_s r\frac{\mathrm{d}x_r}{\mathrm{d}\tau} = y_0 r^2\cos\tau, \tag{7}$$

where ζ_s is the time variable equivalent damping ratio of the MR damper. Applying the transformation

$$x_r = a_r(\tau)\cos\phi(\tau), \qquad \dot{x}_r = -a_r(\tau)\sin\phi(\tau) \tag{8}$$

where $\phi(\tau) = \tau + \varphi$, differentiating x_r with respect to τ, and comparing with equation (8), yields

$$a_r'\cos\phi - a_r\varphi'\sin\phi = 0. \tag{9}$$

Substituting equation (8) into equation (7), combining with equation (9), we have

$$\begin{aligned} 2r^2\frac{\mathrm{d}a_r}{\mathrm{d}\tau} &= a_r\left(1 - r^2\right)\sin 2\phi - 4ra_r\zeta_s\sin^2\phi \\ &- 2y_0r^2\sin\phi\cos(\phi - \varphi) \end{aligned} \tag{10}$$

$$\begin{aligned} 2r^2a_r\frac{\mathrm{d}\varphi}{\mathrm{d}\tau} &= 2a_r\left(1 - r^2\right)\cos^2\phi - 2a_r r\zeta_s\sin 2\phi \\ &- 2y_0r^2\cos\phi\cos(\phi - \varphi). \end{aligned} \tag{11}$$

The function ζ_s is dependent on the control method. For the steady-state response of the system, the values of a_r and φ can be obtained by averaging $\mathrm{d}a_r/\mathrm{d}\tau$ and $\mathrm{d}\varphi/\mathrm{d}\tau$ over one period of time T, or $\phi = [0, 2\pi]$.

Downloaded from jvc.sagepub.com at PENNSYLVANIA STATE UNIV on March 2, 2014

3.1. Steady-state Response of Limited Relative Displacement Control

The control law (1) can be rewritten as

$$\zeta_s = \begin{cases} \zeta_{\max} & 0 < \phi \le \beta \\ 0 & \beta < \phi \le \pi - \beta \\ \zeta_{\max} & \pi - \beta < \phi \le \pi + \beta \\ 0 & \pi + \beta < \phi \le 2\pi - \beta \\ \zeta_{\max} & 2\pi - \beta < \phi < 2\pi \end{cases} \tag{12}$$

where

$$\beta = \arccos\left(\frac{\delta}{a_r}\right). \tag{13}$$

Taking the average of equations (10) and (11), we have

$$\begin{aligned} 2r^2\frac{\mathrm{d}a_r}{\mathrm{d}\tau} &= \frac{1}{2\pi}\int_0^{2\pi}\left[a_r\left(1-r^2\right)\sin 2\phi - 4ra_r\zeta_s\sin^2\phi\right. \\ &- \left. 2y_0r^2\sin\phi\cos(\phi-\varphi)\right]\mathrm{d}\phi \end{aligned} \tag{14}$$

$$\begin{aligned} 2r^2a_r\frac{\mathrm{d}\psi}{\mathrm{d}\tau} &= \frac{1}{2\pi}\int_0^{2\pi}\left[2a_r\left(1-r^2\right)\cos^2\phi - 2a_rr\zeta_s\sin 2\phi\right. \\ &- \left. 2y_0r^2\cos\phi\cos(\phi-\psi)\right]\mathrm{d}\phi. \end{aligned} \tag{15}$$

Integration of the right-hand side of equations (14) and (15) yields

$$\frac{\mathrm{d}a_r}{\mathrm{d}\tau} = -\frac{1}{2\pi r}\left(y_0r\pi\sin\varphi + 4\zeta_{\max}a_r\beta - 2\zeta_{\max}a_r\sin 2\beta\right) \tag{16}$$

$$\frac{\mathrm{d}\varphi}{\mathrm{d}\tau} = -\frac{1}{2a_rr^2}\left(a_rr^2 - a_r + y_0r^2\cos\varphi\right). \tag{17}$$

When the response is at steady state, the amplitude of x_r and the phase φ are assumed constant, which leads to $\mathrm{d}a/\mathrm{d}\tau = 0$ and $\mathrm{d}\varphi/\mathrm{d}\tau = 0$. After eliminating φ from equations and, we have the closed-form frequency response of the system as

$$a_r = \frac{\pi r^2 y_0}{\sqrt{16\zeta_{\max}^2r^2\beta^2\left[1-\sin(2\beta)\right] + \pi^2\left(r^2-1\right)^2 + 4\zeta_{\max}^2r^2\sin^2(2\beta)}} \tag{18}$$

$$\varphi = \tan^{-1}\left[\frac{2\zeta_{\max}r\left[2\beta-\sin(2\beta)\right]}{\pi\left(r^2-1\right)}\right]. \tag{19}$$

Downloaded from jvc.sagepub.com at PENNSYLVANIA STATE UNIV on March 2, 2014

The transmissibility of the relative displacement is

$$\lambda = \left|\frac{a_r}{y_0}\right| = \frac{\pi r^2 y_0}{\sqrt{16\zeta_{\max}^2 r^2\beta^2\left[1-\sin(2\beta)\right] + \pi^2(r^2-1)^2 + 4\zeta_{\max}^2 r^2\sin^2(2\beta)}}. \tag{20}$$

The motion of sprung mass is

$$x_s = x_r + y = a_r\cos(\tau+\varphi) + y_0\cos\tau = a_s\cos(\tau-\varphi_s) \tag{21}$$

where

$$a_s = y_0\sqrt{\left[\frac{2\lambda^2\zeta_{\max}\left[2\beta-\zeta_{\max}\sin(2\beta)\right]}{r\pi}\right]^2 + \left[\frac{\lambda^2+r^2\left(1-\lambda^2\right)}{r^2}\right]^2} \tag{22}$$

$$\varphi_s = \tan^{-1}\left(\frac{4\lambda^2\zeta_{\max} r\left(\beta-\sin\beta\cos\beta\right)}{\pi\left(\lambda^2r^2-\lambda^2-r^2\right)}\right). \tag{23}$$

The acceleration transmissibility of the sprung mass is

$$\eta = \left|\frac{\ddot{x}_s}{y_0\omega_s^2}\right| = r^2\sqrt{\left[\frac{2\lambda^2\zeta_{\max}\left[2\beta-\zeta_{\max}\sin(2\beta)\right]}{r\pi}\right]^2 + \left[\frac{\lambda^2+r^2\left(1-\lambda^2\right)}{r^2}\right]^2}. \tag{24}$$

With equations (20), (24), and (13), we can obtain the system relative displacement transmissibility and acceleration transmissibility shown in Figure 3(a). The figure shows that the averaging method can yield results that are close to the simulation results at the expense of not recovering the high-frequency variation of the frequency response. The frequency response curves of the LRD method are similar to those of a linear system with constant damping ratio. However, the relative displacement of the sprung mass can be controlled by two parameters: δ and $\zeta_{\max}$.

3.2. Steady-state Response of the Modified Skyhook Control Method

Similar to Section 3.1, assuming $x_r = a_r\cos(\tau+\varphi) = a_r\cos\phi$, we then have

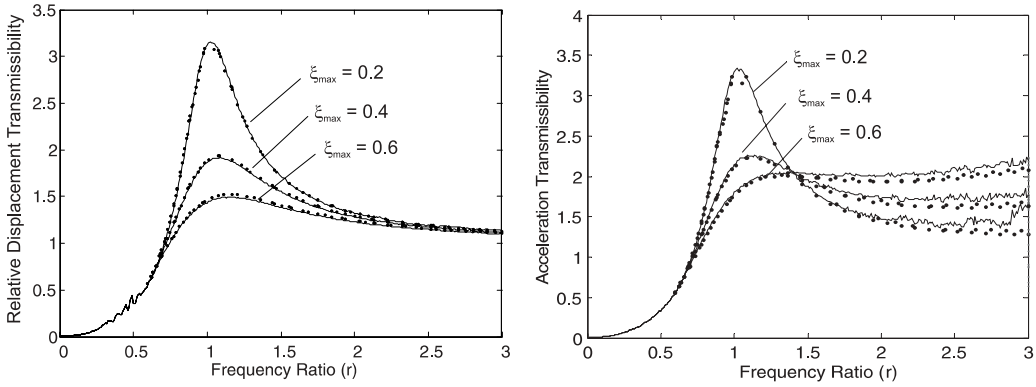
$$x_s = x_r + y = a_s\cos(\tau+\beta) = a_s\cos(\phi+\alpha) \tag{25}$$

where

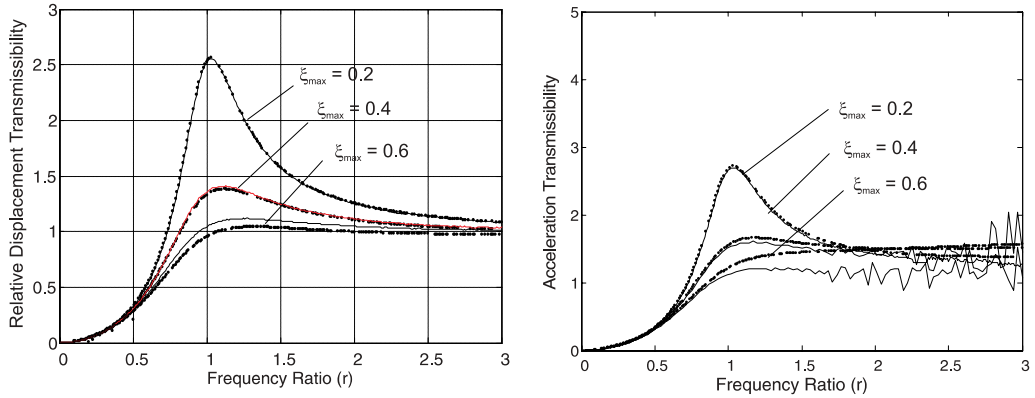
$$\beta = \tan^{-1}\left(\frac{a_r\sin\varphi}{a_r\cos\varphi + y_0}\right)$$
$$\alpha = \beta - \varphi. \tag{26}$$

If a_s and β are slowly varied, we have

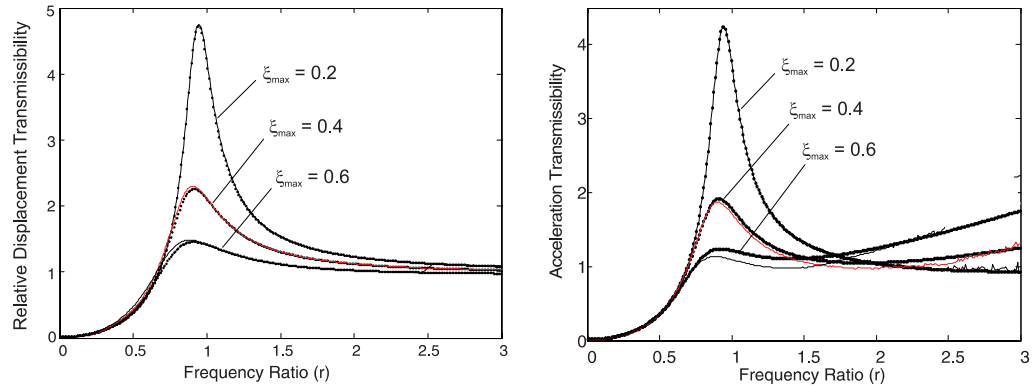
Downloaded from jvc.sagepub.com at PENNSYLVANIA STATE UNIV on March 2, 2014



(a) Limited relative displacement control ($\delta = 0.5\ y_0$)



(b) Modified skyhook control method



(c) R-S control method

Figure 3. Comparison of the averaging results with numerical simulation results for different control methods: dotted line, averaging method; solid line, numerical simulation results.

Downloaded from jvc.sagepub.com at PENNSYLVANIA STATE UNIV on March 2, 2014

$$\begin{aligned} \dot{x}_s &\approx -a_s\omega\sin(\omega t+\beta) = -a_s\omega\sin(\tau+\alpha) \\ \ddot{x}_s &\approx a_s\omega^3\sin(\omega t+\beta) = a_s\omega^3\sin(\tau+\alpha). \end{aligned} \tag{27}$$

Therefore, the jerk and absolute velocity of the sprung mass have an approximation of opposite sign and the phase α can be approximately regarded as a constant. According to the control strategy described in equation (2), it can be rewritten in the form

$$\zeta_s = \begin{cases} \zeta_{\max} & 0 < \phi \le \pi - \alpha \\ 0 & \pi - \alpha < \phi \le \pi \\ \zeta_{\max} & \pi < \phi \le 2\pi - \alpha \\ 0 & 2\pi - \alpha < \phi \le 2\pi\,. \end{cases} \tag{28}$$

Substituting equation (28) into equations (10) and(11) , and performing the averaging calculation, yields

$$\frac{\mathrm{d}a_r}{\mathrm{d}\tau} = -\frac{2\zeta_{\max}a_r\,(\pi-\alpha)+\zeta_{\max}a_r\sin(2\alpha)+y_0\pi r\sin\varphi}{2\pi r} \tag{29}$$

$$\frac{\mathrm{d}\varphi}{\mathrm{d}\tau} = -\frac{a_r\pi\left(r^2-1\right)+2\zeta_{\max}ra_r\sin^2\alpha+y_0\pi r^2\cos\varphi}{2\pi a_r r^2}. \tag{30}$$

By setting $\mathrm{d}a_r/\mathrm{d}\tau$ and $\mathrm{d}\varphi/\mathrm{d}\tau$ equal to zero, the steady-state response of the system can be obtained by combining equations (29) and (30) with the following equations:

$$\begin{aligned} \alpha &= \beta-\varphi, \\ \sin\beta &= \frac{a_r\sin\varphi}{\sqrt{(a_r\cos\varphi+y_0)^2+(a_r\sin\varphi)^2}}, \\ \cos\beta &= \frac{a_r\cos\varphi+y_0}{\sqrt{(a_r\cos\varphi+y_0)^2+(a_r\sin\varphi)^2}}. \end{aligned} \tag{31}$$

Since equations (29)–(31) are nonlinear equations, the values of a_r and φ for a varied frequency ratio must be obtained by numerical methods. The procedure can be described as

$$\text{Minimize}\left[\left(\frac{\mathrm{d}a_r}{\mathrm{d}\tau}\right)^2+\left(\frac{\mathrm{d}\varphi}{\mathrm{d}\tau}\right)^2\right] \tag{32}$$

to obtain a_r and φ under the condition $a_r \ge 0$ and $0 \le \varphi < 2\pi$.

Since $x_s = x_r + y_0\cos\tau$, after some deduction, we have

$$\lambda = \left|\frac{a_r}{y_0}\right|$$

Downloaded from jvc.sagepub.com at PENNSYLVANIA STATE UNIV on March 2, 2014

$$\eta = \left| \frac{\ddot{x}_s}{y_0 \omega_s^2} \right| = r^2 \sqrt{\lambda^2 \sin^2 \varphi + (\lambda \cos \varphi + 1)^2}. \tag{33}$$

Comparisons of the relative displacement and the acceleration transmissibility are shown in Figure 3(b). This shows that the acceleration transmissibility at high frequencies increases slightly when the damping ratio is increased. As a result, the MSK method can maintain good ride quality while the relative displacement is decreased.

3.3. Steady-state Response of the Rakheja–Sankar Control Method

The control strategy described in equation (5), can be expressed in the following form:

$$\zeta_s = \begin{cases} \zeta_{\max} & x_r \dot{x}_r \leq 0 \\ 0 & x_r \dot{x}_r > 0. \end{cases} \tag{34}$$

Over a period of time, the control strategy (34) can be rewritten as

$$\zeta_s = \begin{cases} \zeta_{\max} & 0 < \phi \leq \pi/2, \quad \pi < \phi \leq 3\pi/2 \\ 0 & \pi/2 < \phi \leq \pi, \quad 3\pi/2 < \phi \leq 2\pi. \end{cases} \tag{35}$$

Averaging equations (10) and (11) over one period yields

$$\begin{aligned} \frac{\mathrm{d}a_r}{\mathrm{d}\tau} &= -\frac{1}{2r} \left(y_0 r \sin \varphi + a_r \zeta_{\max} \right) \\ \frac{\mathrm{d}\varphi}{\mathrm{d}\tau} &= \frac{1}{2\pi a_r r^2} \left[\pi a_r \left(1 - r^2 \right) - \pi y_0 r^2 \cos \varphi - 2\zeta_{\max} r a_r \right]. \end{aligned} \tag{36}$$

Considering a_r and φ as constant, i.e. $\mathrm{d}a_r/\mathrm{d}\tau$ and $\mathrm{d}\varphi/\mathrm{d}\tau$ equal to zero, leads to

$$\lambda = \left| \frac{a_r}{y_0} \right| = \frac{\pi r^2}{\sqrt{(4 + \pi^2) r^2 \zeta_{\max}^2 + 4\pi r (r^2 - 1) \zeta_{\max} + \pi (r^2 - 1)^2}} \tag{37}$$

$$\varphi = \tan^{-1} \left[\frac{\zeta_{\max} r \pi}{\pi \left(r^2 - 1 \right) + 2\zeta_{\max} r} \right]. \tag{38}$$

The acceleration of the mass is

$$x_s = a_s \cos(\tau - \varphi_s) \tag{39}$$

where

$$a_s = \sqrt{\left(\frac{\zeta_{\max} \lambda^2}{r} \right)^2 + \left(1 - \lambda^2 + \frac{\lambda^2}{r^2} - \frac{2\lambda^2 \zeta_{\max}}{r\pi} \right)^2} \tag{40}$$

Downloaded from jvc.sagepub.com at PENNSYLVANIA STATE UNIV on March 2, 2014

$$\varphi_s = -\tan^{-1}\left[\frac{\pi\zeta_{\max}\lambda^2 r}{\pi r^2\left(\lambda^2-1\right)+\lambda^2\left(2\zeta_{\max}r-\pi\right)}\right] \tag{41}$$

and the acceleration transmissibility of the sprung mass is

$$\eta = \left|\frac{\ddot{x}_s}{y_0\omega_s^2}\right| = r^2\sqrt{\left(\frac{\zeta_{\max}\lambda^2}{r}\right)^2+\left(1-\lambda^2+\frac{\lambda^2}{r^2}-\frac{2\lambda^2\zeta_{\max}}{r\pi}\right)^2}. \tag{42}$$

Figure 3(c) shows that the R–S control method has a good isolation performance in the high-frequency region, except that it has a relatively higher acceleration transmissibility around the natural frequency than the case when the system has a constant damping ratio. Since this controller only needs one sensor, it is a practical control method for suspension real time control.

3.4. Vibration Control Efficiency Comparison

Using the averaging method, we have obtained the sprung mass relative displacement and acceleration transmissibilities for different control methods. When the damper has a constant damping ratio, the relative displacement transmissibility λ and acceleration transmissibility η of 1DOF suspension system can be written in the form:

$$\begin{aligned}\lambda &= \left|\frac{x_r}{y}\right| = \frac{r^2}{\sqrt{(1-r^2)^2+(2\zeta_s r)^2}}\\ \eta &= \left|\frac{\ddot{x}_s}{\omega_s^2 y}\right| = \frac{r^2\sqrt{1+(2\zeta_s r)^2}}{\sqrt{(1-r^2)^2+(2\zeta_s r)^2}}.\end{aligned} \tag{43}$$

Taking the root-mean-square (RMS) values of λ and η from equation (43) and the other three proposed semi-active control methods, we can compare the vibration control efficacy of the different control methods. The RMS of λ and η can be calculated from

$$\begin{aligned}\lambda_{RMS} &= \sqrt{\frac{1}{(r_{\max}-r_{\min})}\sum_{r_{\min}}^{r_{\max}}\lambda^2\Delta r}\\ \eta_{RMS} &= \sqrt{\frac{1}{(r_{\max}-r_{\min})}\sum_{r_{\min}}^{r_{\max}}\eta^2\Delta r}.\end{aligned} \tag{44}$$

When $r_{\max}=3$, $r_{\min}=0$, the RMS values of λ versus η for different control methods are shown in Figure 4. In the figure, the R–S control is represented by a smooth curve, in comparison to MSK and LRD data points, because it was extracted from a closed-form solution. The results of the MSK and LRD control methods are obtained by solving nonlinear algebraic equations numerically. The figure shows that the R–S control method has the lowest RMS acceleration when compared with the other control methods. The MSK method also

Downloaded from jvc.sagepub.com at PENNSYLVANIA STATE UNIV on March 2, 2014

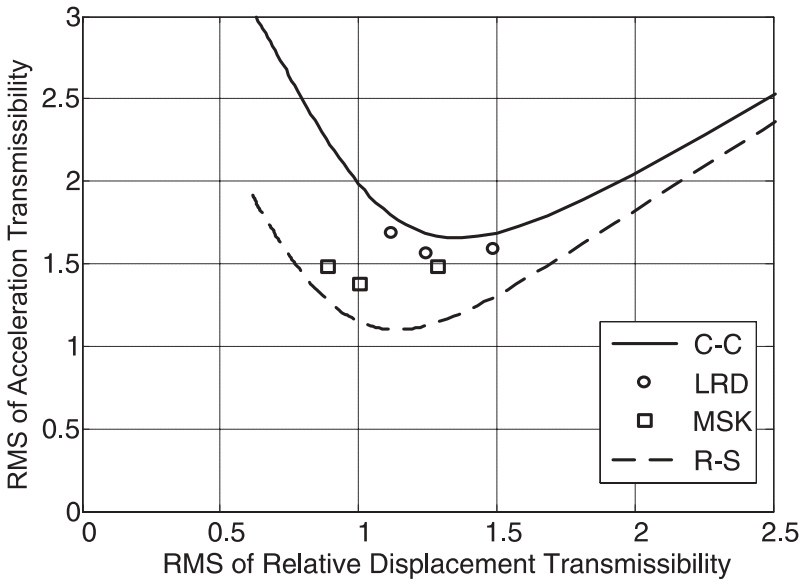


Figure 4. Analytical comparison of semi-active control methods with constant damping cases: CC, constant damping case; LRD, limited relative displacement control; MSK, modified skyhook control; R–S, R–S control method.

has a good vibration control efficacy. However, the LRD method has an RMS acceleration that is very close to the case of constant damping.

4. EXPERIMENTAL VERIFICATION

To verify the control efficacy of the different control methods, a suspension test facility has been developed, as shown in Figure 5. In this test facility, a 1DOF suspension is mounted on an LMS722 shaker. The suspension system has a 5.70 kg sprung mass and total stiffness of 18.90 kN m^{-1}. The natural frequency of the system is 57.60 rad s^{-1} (9.17 Hz). A sponge-based MR damper (RD-1097-01) was adopted to provide the damping force to the system. This type of damper has the advantages of requiring no seals or bearings, being low cost, and having a compact structure. It should be emphasized that the damping force provided by the MR damper is a hysteretic damping force, instead of a liner damping force as we have used to obtain the analytical results in Section 3. However, Shen et al. (2005) have compared the results of the averaging method with the experimental results of a 1DOF system with the same MR damper and have shown that the analytical results and experimental results agree well. Therefore, it is still valid to compare the theoretical and experimental results for the different control methods.

In the test facility, three sensors are used to measure the response of the system. A load cell (Sensotec Model 41) was used to measure the damping force on the sprung mass, an LVDT (RDP Group LDC 500C) was used to measure the relative displacement of the sprung

Downloaded from jvc.sagepub.com at PENNSYLVANIA STATE UNIV on March 2, 2014

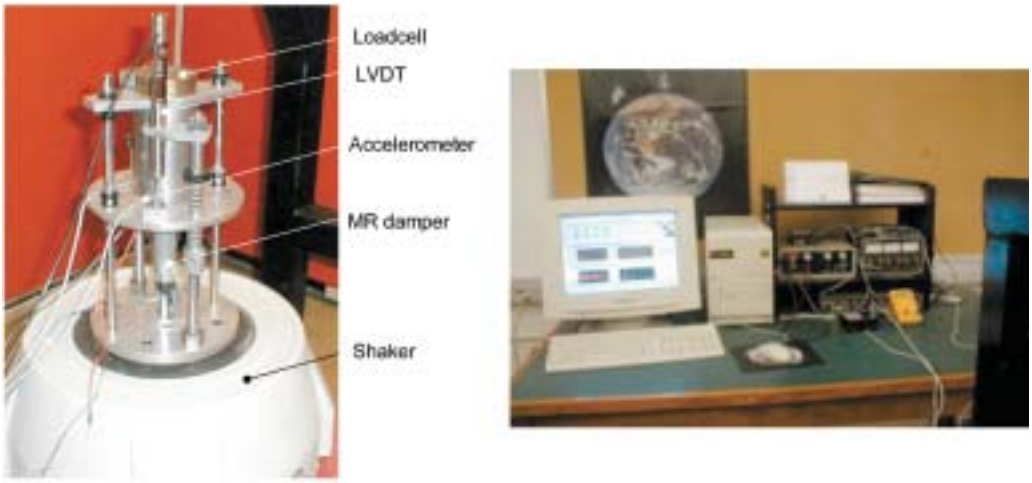


Figure 5. Quarter-car model suspension test rig.

mass, and two accelerometers (Dytran 3035AG) were used to measure the acceleration of the sprung mass and the base. The measured signals are sampled by a PCI-DAS 1602/16 multifunction A/D–D/A I/O board and were selected as feedback control signals for the different control methods.

4.1. Implementation of the Control Methods

4.1.1. Limited Relative Displacement Control Method

The LRD method implementation is described in Figure 6(a), where it is illustrated how the measured relative displacement is first filtered with a high-pass filter that has a 4 rad s^{-1} pass-band edge to eliminate the offset of the signal. Then, the signal noise is filtered with a low-pass filter that has a 80π rad s^{-1} pass-band edge. The parameter δ is taken to be 0.51 mm. This control method only needs one feedback signal and it is possible to set up the LRD system at low cost.

4.1.2. Modified Skyhook Control Method

The MSK method is described in Figure 6(b), where two low-pass filters with a pass-band edge frequency of 80π rad s^{-1} are used to condition the measured signal. For this control method, the relative displacement and acceleration are used as feedback signals. Here we use $\ddot{x}_s$ instead of $\dot{x}_s$ to determine the velocity direction of the sprung mass. Since the value of $\ddot{x}_s$ can be easily obtained by differentiating the filtered sprung mass acceleration $\ddot{x}_s$, it makes this method more practical than the traditional MSK method, which, as discussed above, needs to determine the sprung mass velocity by designing a complicated observer or by integrating the acceleration. Since the acceleration differentiation brings noise to the signal, a post low-pass filter is needed.

Downloaded from jvc.sagepub.com at PENNSYLVANIA STATE UNIV on March 2, 2014

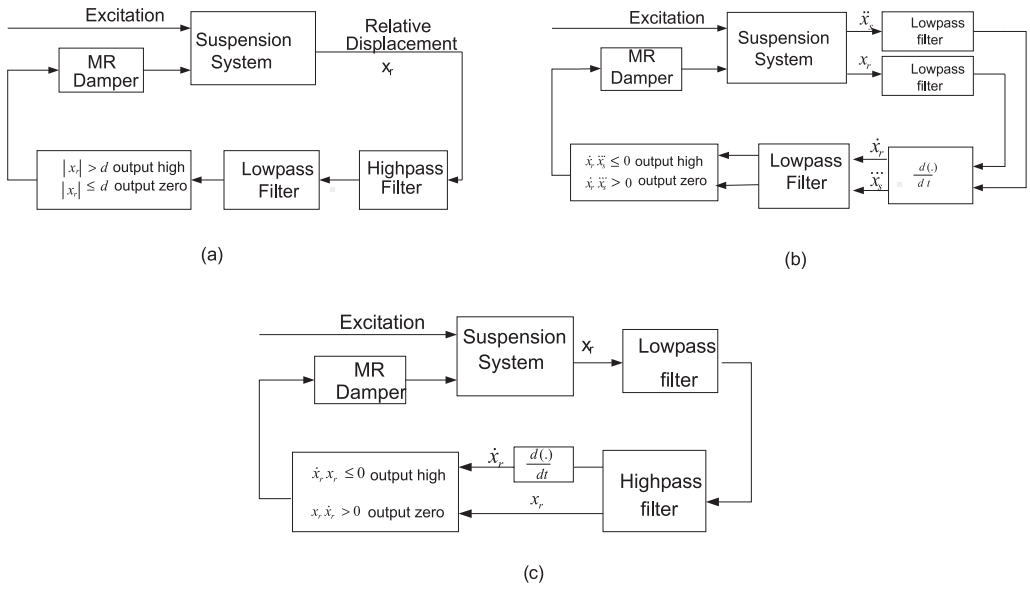


Figure 6. Schematic diagrams of different control methods in the test rig: (a) limited relative displacement control method; (b) modified skyhook control method; (c) R–S control method.

4.1.3. Modified Rakheja–Sankar Control Method

The modified R–S control method is schematically shown in Figure 6(c). This control method also only needs one feedback signal, the relative displacement of the sprung mass to the base. The high-pass filter and low-pass filters are used to condition the signal.

4.2. Experimental Results

In order to compare the performance of the different control methods, two different excitations were employed: one was a swept sine excitation and the other a random excitation. To assess the above three semi-active control methods, the responses of the sprung mass under constant damping are used as a reference. For all three on–off controllers, the damper is applied a serious value of current for the on state and zero current to the MR damper for the off state.

4.2.1. Swept Sine Excitation

For the swept sine excitation vibration test, the drive signal to the shaker was a sine wave that had excitation amplitude of 0.6 mm, and the excitation frequency was gradually increased from 5 to 30 Hz over 5 min. The 5 Hz minimum test frequency is the physical limitation of the shaker. The acceleration and relative displacement of the sprung mass were recorded and processed with a fast Fourier transform to obtain the frequency response of the system.

Downloaded from jvc.sagepub.com at PENNSYLVANIA STATE UNIV on March 2, 2014

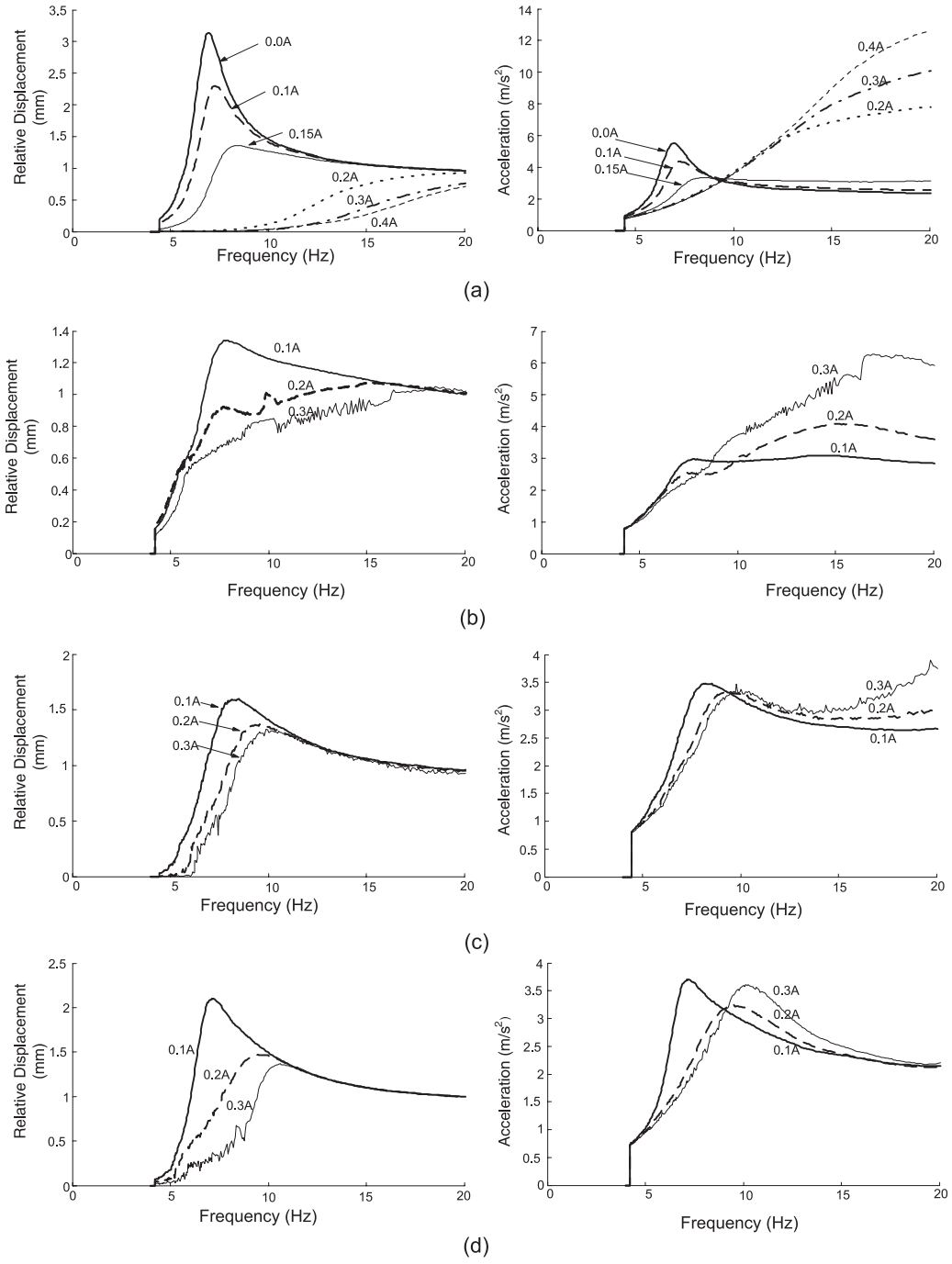


Figure 7. Experimental results of different control methods: (a) constant currents; (b) limited relative displacement; (c) modified skyhook control; (d) R–S control.

Downloaded from jvc.sagepub.com at PENNSYLVANIA STATE UNIV on March 2, 2014

Table 1. RMS of sprung mass response when the damper is applied a series of constant current (CC) (swept sine excitation $y = \sin(\omega t)$ mm).

Applied current	0.0A	0.1A	0.15A	0.2A	0.3A	0.4A
RMS of relative disp. (mm)	1.2885	1.1192	0.9069	0.4970	0.3162	0.2682
RMS of acceleration ($m\,s^{-2}\,Hz^{-1}$)	2.6165	2.5256	2.5759	4.7868	5.5602	6.5097

When the MR damper was applied a series of constant currents, the frequency responses of the system are shown in Figure 7(a). These experimental results serve as a reference to evaluate the semi-active control methods.

The frequency responses of the proposed three semi-active control methods are shown in Figures 7 (b)–(d). From these figures, we can conclude the following.

1) For the LRD method, the small relative displacement is corresponds to a high sprung mass acceleration in the high-frequency range.
2) The MSK method can achieve a lower sprung mass acceleration than the LRD method when the maximum voltage applied to the MR damper is varied from a low value to a high value. However, the acceleration frequency response of the SKC method has a large variation. This can be explained as the result of the filtered acceleration still having too much noise, which causes the jerk of the sprung mass to have a large variation too. This may also cause the controller to misjudge the direction of the sprung mass absolute velocity. However, it still has good vibration isolation performance.
3) The experimental results show that the R–S control can obtain a low sprung mass acceleration while keeping the relative displacement small.

The RMS values of the sprung mass relative displacement and acceleration are calculated from

$$\begin{aligned} (x_r)_{RMS} &= \sqrt{\frac{1}{25}\sum_{freq=5}^{freq=30}(x_r)_{freq}^2\Delta_{freq}} \\ (\ddot{x}_s)_{RMS} &= \sqrt{\frac{1}{25}\sum_{freq=5}^{freq=30}(\ddot{x}_s)_{freq}^2\Delta_{freq}}. \end{aligned} \tag{45}$$

Tables 1 and 2 show the calculation results for the cases when the MR damper is applied different constant currents and the three semi-active control methods. Figure 8 shows the RMS acceleration versus RMS relative displacement for the different control methods. In the figure, the reference curve is obtained by connecting all the RMS points corresponding to the cases where a constant voltage has been applied to the MR damper. From Figure 8, we find that the R–S method and the MSK method can provide good vibration isolation performance, especially the R–S control method. For the same relative displacement, the R–S control can achieve a much smaller value of acceleration than the constant voltage cases. However, the LRD method has not improved the ride comfort, although it does control the sprung mass relative displacement very well.

Downloaded from jvc.sagepub.com at PENNSYLVANIA STATE UNIV on March 2, 2014

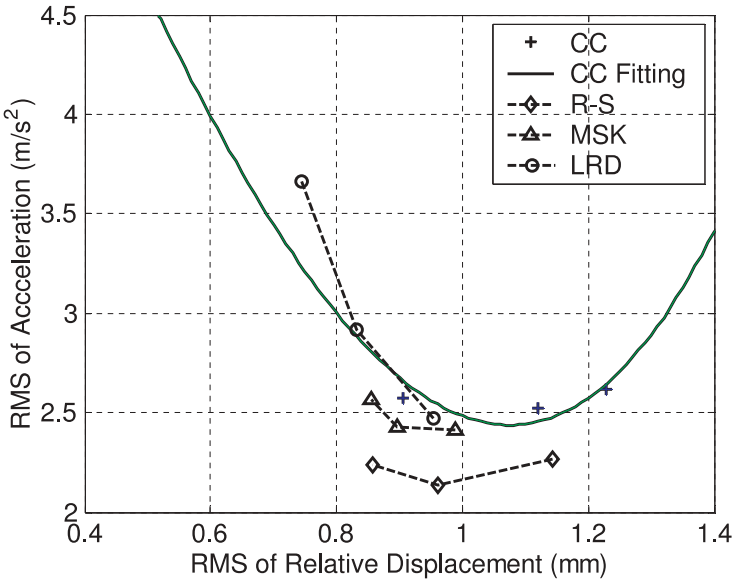


Figure 8. Comparison of semi-active control methods with constant damping cases (swept sine excitation $y = 0.6\sin(\omega t)$ (mm)).

Table 2. RMS of sprung mass response for different control methods (swept sine excitation $y = \sin(\omega t)$ mm).

Control method	LRD control			MSK control			R–S control		
"on state" applied current	0.1 A	0.2A	0.3A	0.1A	0.2A	0.3A	0.1A	0.2A	0.3A
Relative disp. (mm)	0.9541	0.18324	0.7439	0.9895	0.8961	0.8541	1.1421	0.9605	0.8575
Acceleration (m/s^2)	2.4685	2.9142	3.6628	2.415	2.4277	2.5678	2.2693	2.1369	2.2407

4.2.2. Random Excitation

For random excitation, the random power spectral density (PSD) profile can be described as follows.

The excitation frequency has a minimum frequency of 5 Hz and a maximum frequency of 30 Hz. The acceleration PSD value at 5 Hz is 0.07 (m s^{-2})^2 Hz^{-1}. The starting slope of the PSD is 6.80dB oct^{-1} and the acceleration value of the PSD at 30 Hz is 4 (m s^{-2})^2 Hz^{-1}. Figure 9 shows a sample of the base acceleration in the time domain.

Downloaded from jvc.sagepub.com at PENNSYLVANIA STATE UNIV on March 2, 2014

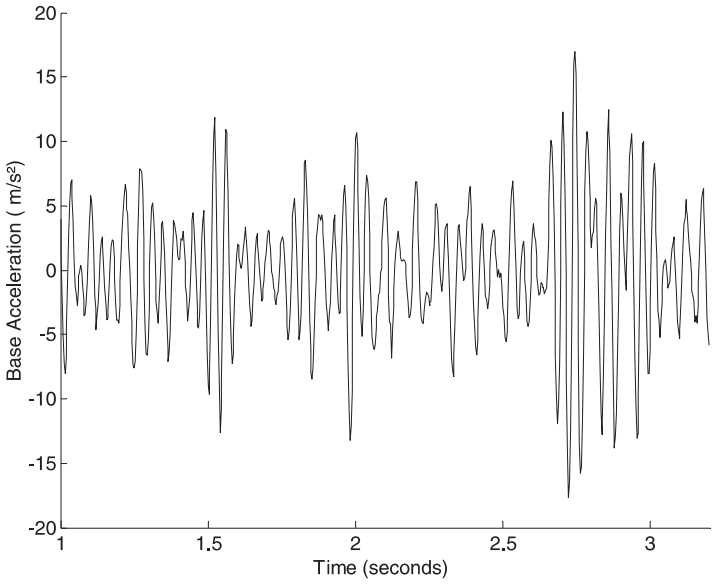


Figure 9. The base excitation of the suspension in time domain.

Table 3. RMS of sprung mass response (random excitation, 5–30Hz).

	CC 0.0A	CC 0.1A	CC 0.2A	CC 0.3A	CC 0.4A	LRD 4v	LRD 8v	MSK 4v	MSK 8v	R–S 4v	R–S 8v
Relative disp. $(mm)^2/Hz$	0.054	0.0466	0.0217	0.0150	0.0082	0.0357	0.0253	0.0381	0.0277	0.0352	0.0197
Acceleration $(m/s^2)^2/Hz$	0.8233	0.8618	0.8409	1.027	1.616	0.8291	0.8499	0.7812	0.8135	0.8056	0.8204

When the MR damper is actuated with a series of constant current values, the PSDs of the relative displacement and acceleration of the sprung mass are shown in Figure 10(a). For the proposed three semi-active control methods, the PSDs of the relative displacement and acceleration are shown in Figure 10(b). The RMS of the sprung mass relative displacement and acceleration can be calculated with equation (45). The calculation results are listed in Table 3.

To evaluate the performance of the different control methods under random excitation, comparisons of the RMS of the relative displacement versus acceleration for different control methods are shown in Figure 11. The comparisons show that different control methods have a similar performance for both swept sine excitation and random excitation. The modified R–S control method and the modified SKC method have good vibration control properties when compared to the constant current actuated MR damper and when we regard ride comfort corresponding to same RMS relative displacement.

Downloaded from jvc.sagepub.com at PENNSYLVANIA STATE UNIV on March 2, 2014

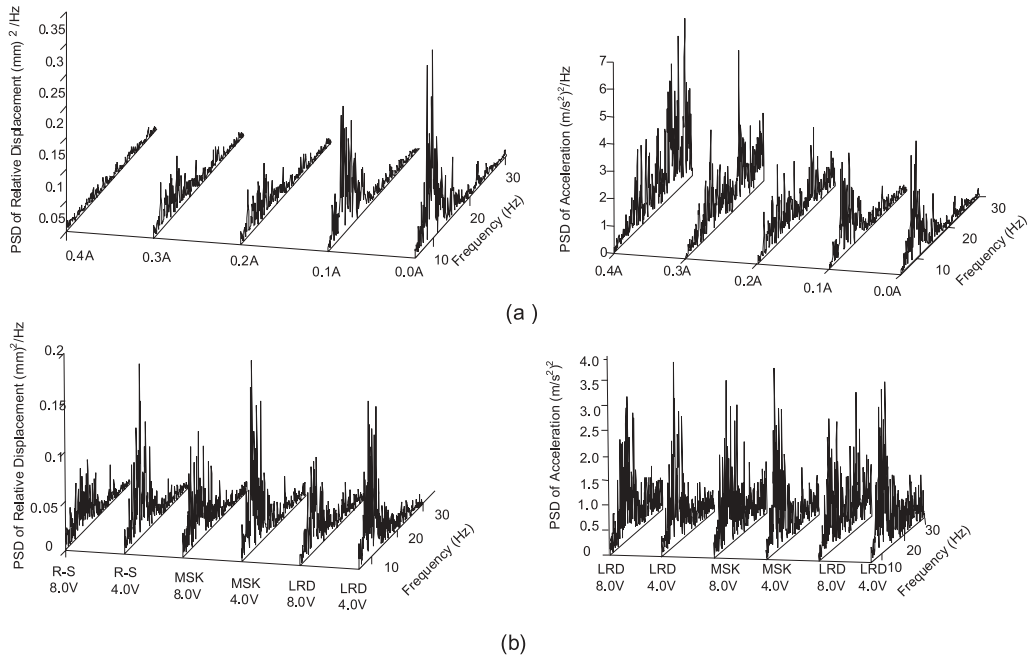


Figure 10. Comparison of PSDs of different control methods under random excitation.

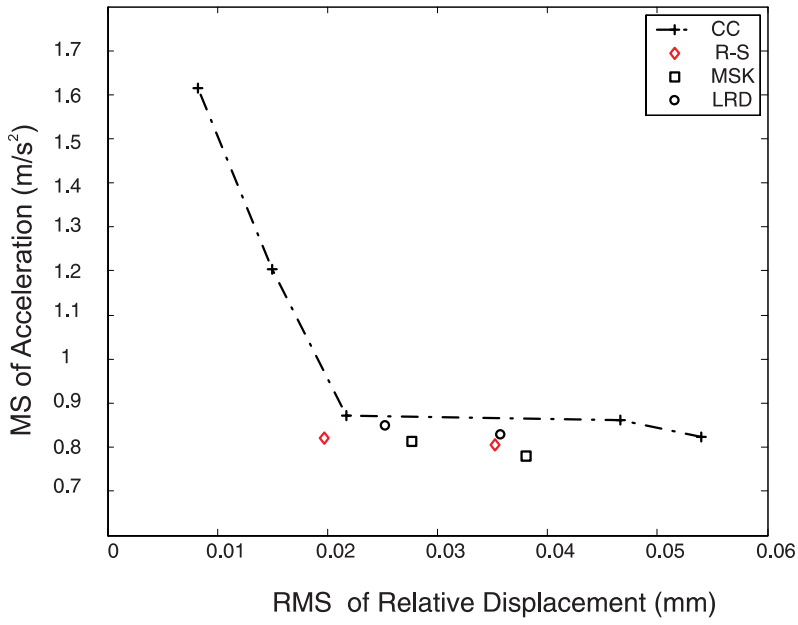


Figure 11. Experimental comparison of semi-active control methods with constant damping cases (random excitation).

Downloaded from jvc.sagepub.com at PENNSYLVANIA STATE UNIV on March 2, 2014

5. CONCLUSIONS

Three semi-active control methods have been proposed and analyzed. The averaging method has been used to investigate the performance of different control methods. The numerical simulation results show that the averaging method provides a good approximation of the system response for different control methods. An experimental facility has been used to verify the efficiency of the different control methods by exciting the system with either swept sine or random excitations. The experimental results show that the modified R–S method and the MSK method provide better ride comfort compared with the results obtained by using constant damping obtained by applying a constant voltage to the MR. The limited relative displacement method can adjust the maximum relative displacement of the system easily; however, it does not evidently improve the ride quality of the system. The R–S control method is highly recommended, for it needs only one sensor and produces good vibration control performance. The MSK method used in this paper is also a practical control method. In the MSK method, the jerk of the sprung mass has been used to indirectly determine the direction of sprung mass absolute velocity. This method may simplify the application of the MSK method to a suspension system.

The experimental results show that the R–S control method and MSK method can be easily applied to a real system and have better vibration control capability than by applying a constant current (or voltage) to the MR damper of the system. The LRD control can effectively control the relative displacement of the sprung mass by setting its control parameters. However, it does not improve the ride comfort much from analytical and experimental results.

REFERENCES

Alanoly, J. and Sankar, S., 1987, "A new concept in semi-active vibration isolation," *Journal of Mechanisms, Transition, and Automation in Design* **109**(2), 242–247.

Boggs, C. M., Goncalves, F. D., and Ahmadian, M., 2004, "Steady-state energy transfer of a semi-active suspension under hybrid control," *Proceedings of the ASME Design Engineering Division* **117,** 757–765.

Choi, S. B., Lee, H. K., and Chang, E. G., 2001, "Field test results of a semi-active ER suspension system associated with skyhook controller," *Mechatronics* **11**, 345–353

Dyke, S. J., Spencer, B. F. Jr., Sain, M. K., and Carlson, J. D., 1998, "An experimental study of MR dampers for seismic protection," *Smart Materials and Structures* **7**, 693–703.

Hedrick, J. K., Rajamani, R., and Yi, K., 1994, "Observer design for electronic suspension applications," *Vehicle System Dynamics* **23**, 413–440.

Hrovat, D., Margolis, D. L., and Hubbard, M., 1988, "An approach toward the optimal semi-active suspension," *Journal of Dynamic Systems, Measurement, and Control* **110**, 288–296.

Kim, J. H. and Lee, C. W., 2003, "Semi-active damping control of suspension system for specified operational response mode," *Journal of Sound and Vibration* **260**, 307–328.

Lai, C. Y. and Liao, W. H., 2002, "Vibration control of a suspension system via a manetorheological fluid damper," *Journal of Vibration and Control* **8**, 527–547.

Leitmann, G., 1995, "A control scheme based on ER-materials for vibration attenuation of dynamical system," *Applied Mathematics and Computation* **70**, 247–259.

Rabinow, J., 1948, "The magnetic fluid clutch," *AIEE Transactions* **67**, 1308–1315.

Rakheja, S. and Sankar, S., 1985, "Vibration and shock isolation performance of a semi-active on–off damper," *Journal of Vibration, Acoustics, Stress, and Reliability in Design* **107**(4), 398–403.

Downloaded from jvc.sagepub.com at PENNSYLVANIA STATE UNIV on March 2, 2014

Shen, Y., Golnaraghi, M. F., and Heppler, G. R., 2005, "Analytical and experimental study of the response of a suspension system with a magnetorheological damper," *Journal of Intelligent Material Systems and Structures* **16,** 135–147**.**

Yao, G. Z., Yap, F. F., Chen, G., Li, W. H., and Yeo, S. H., 2002, "MR damper and its application for semi-active control of vehicle suspension system," *Mechatronics* **12**, 963–973.

Downloaded from jvc.sagepub.com at PENNSYLVANIA STATE UNIV on March 2, 2014